



UNIVERSITY
OF WOLLONGONG
AUSTRALIA

University of Wollongong
Research Online

Faculty of Engineering - Papers (Archive)

Faculty of Engineering and Information Sciences

2012

Structural dependent ultrafast electron-phonon coupling in multiferroic BiFeO₃ films

Zuanming Jin
Shanghai University

Yue Xu
Shanghai University

Zhengbing Zhang
Shanghai University

Gaofang Li
Shanghai University

Xian Lin
Shanghai University

See next page for additional authors

<http://ro.uow.edu.au/engpapers/5086>

Publication Details

Jin, Z., Xu, Y., Zhang, Z., Li, G., Lin, X., Ma, G., Cheng, Z. & Wang, X. (2012). Structural dependent ultrafast electron-phonon coupling in multiferroic BiFeO₃ films. *Applied Physics Letters*, 100 (7),

Research Online is the open access institutional repository for the University of Wollongong. For further information contact the UOW Library:
research-pubs@uow.edu.au

Authors

Zuanming Jin, Yue Xu, Zhengbing Zhang, Gaofang Li, Xian Lin, Guohong Ma, Zhenxiang Cheng, and Xiaolin Wang

Structural dependent ultrafast electron-phonon coupling in multiferroic BiFeO₃ films

Zuanming Jin, Yue Xu, Zhengbing Zhang, Gaofang Li, Xian Lin et al.

Citation: *Appl. Phys. Lett.* **100**, 071105 (2012); doi: 10.1063/1.3685496

View online: <http://dx.doi.org/10.1063/1.3685496>

View Table of Contents: <http://apl.aip.org/resource/1/APPLAB/v100/i7>

Published by the American Institute of Physics.

Related Articles

Electrically driven metal-insulator switching in δ -KxV₂O₅ nanowires

Appl. Phys. Lett. **101**, 163502 (2012)

Heteroepitaxial VO₂ thin films on GaN: Structure and metal-insulator transition characteristics

J. Appl. Phys. **112**, 074114 (2012)

Investigation of nonuniformity phenomenon in nanoscale SiO₂ and high-k gate dielectrics

J. Appl. Phys. **112**, 064119 (2012)

Strain dependent stabilization of metallic paramagnetic state in epitaxial NdNiO₃ thin films

Appl. Phys. Lett. **101**, 132101 (2012)

Electrical and optical properties of vanadium dioxide containing gold nanoparticles deposited by pulsed laser deposition

Appl. Phys. Lett. **101**, 133102 (2012)

Additional information on *Appl. Phys. Lett.*

Journal Homepage: <http://apl.aip.org/>

Journal Information: http://apl.aip.org/about/about_the_journal

Top downloads: http://apl.aip.org/features/most_downloaded

Information for Authors: <http://apl.aip.org/authors>

ADVERTISEMENT



ACCELERATE COMPUTATIONAL CHEMISTRY BY 5X.
TRY IT ON A FREE, REMOTELY-HOSTED CLUSTER.

LEARN MORE

Structural dependent ultrafast electron-phonon coupling in multiferroic BiFeO₃ films

Zuanming Jin,¹ Yue Xu,¹ Zhengbing Zhang,¹ Gaofang Li,¹ Xian Lin,¹ Guohong Ma,^{1,a)} Zhenxiang Cheng,^{2,a)} and Xiaolin Wang²

¹Department of Physics, Shanghai University, 99 Shangda Road, Shanghai 200444, People's Republic of China

²Institute for Superconductor and Electronic Materials, University of Wollongong, Squair Ways, North Wollongong, NSW 2500, Australia

(Received 10 January 2012; accepted 30 January 2012; published online 15 February 2012)

The electronic energy relaxation of polycrystalline BiFeO₃ films is studied using ultrafast pump-probe spectroscopy. After photo-excitation with femtosecond laser pulses, the relaxation of hot electrons is identified to decay with two different characteristic times. The fast process is attributed to scattering of electrons with lattice-vibration modes, and the slow one is corresponding to the spin-lattice thermalization. The electron-phonon coupling is characterized by the second moment of the Eliashberg function, $\lambda\langle\omega^2\rangle$. Due to the structural strain and symmetry breaking, the electron-phonon interaction strength of tetragonal BiFeO₃ films is larger than that of rhombohedral counterparts. © 2012 American Institute of Physics. [doi:10.1063/1.3685496]

Single phase multiferroic material, BiFeO₃ (BFO), is found in a G-type antiferromagnetic state with $T_N \sim 640$ K, ferroelectric Curie temperature $T_C \sim 1100$ K, and exhibits a weak ferromagnetism at room temperature.^{1–3} Due to large ferroelectric polarization of $\sim 100 \mu\text{C}/\text{cm}^2$, magneto-electric coupling, and the possibility of epitaxial strain engineering of magneto-electric properties, BFO has attracted enormous attention.^{4–7} Recently, a tetragonal BFO has been of great interest, not only as it potentially possesses a giant polarization and enhanced electromechanical response,⁸ but also it provides a unique example of a concurrent magnetic and ferroelectric transition at near room temperature.⁹ From the applied point of view in photonics, it has been proposed that terahertz radiation from BFO films can be used in ferroelectric domain imaging and optical readout of the state of ferroelectric memories.^{10,11} In addition, due to high optical transparency and large third order optical nonlinearities, BFO films are promising for applications in ultrafast photonic devices.^{12,13}

No matter the structural dependent emission of THz radiation or the nonlinear photonic devices, a detailed understanding of the interaction of electron and lattice over a picosecond time scale is an indispensable issue,¹⁴ which is decisive for determining the functional properties of materials. Transient reflectivity changes related to the temporal evolution of the dielectric constant $\Delta\epsilon$ is a direct signature of the electron-phonon (e-ph) energy relaxation process with sub-picosecond resolution. Detailed experimental data of e-ph relaxation process have not been systematically studied in multiferroic materials, though the relevant investigations have been collected for metals,^{15,16} metal nanostructures,¹⁷ graphite,¹⁸ and high-temperature superconductors.^{19–22} In this letter, the time-resolved pump-probe technique is employed to investigate the electronic energy relaxation in multiferroic BFO films. The sub-picosecond bi-exponential

decay is identified as the recovery of photo-excited hot electrons via e-ph and spin-phonon (s-ph) relaxation processes. It is demonstrated experimentally that the e-ph energy relaxation times (τ_{e-ph}) of the tetragonal BFO films are faster compared to that of the rhombohedral ones, which suggests that e-ph interaction is enhanced by structure strain and symmetry breaking in tetragonal BFO films.

To develop high quality BFO films for applications, epitaxial strains from the substrate have been widely used to tune the crystal phase and the physical behavior, which is known as “strain engineering”.²³ The BFO epitaxial thin films could be stabilized in several different crystal structure systems, including monoclinic, tetragonal, rhombohedral, and orthorhombic arrangements.²⁴ The BFO films used in the present study are deposited on the SrTiO₃ (STO) and yttrium stabilized ZrO₂ (YSZ) substrates, respectively, by a pulsed laser deposition system with a 355 nm Nd:YAG laser source at a repetition rate of 10 Hz. The deposition was carried out at 600 °C with a dynamic oxygen pressure of 20 mtorr. The film thickness is about 150 nm. Figure 1 shows

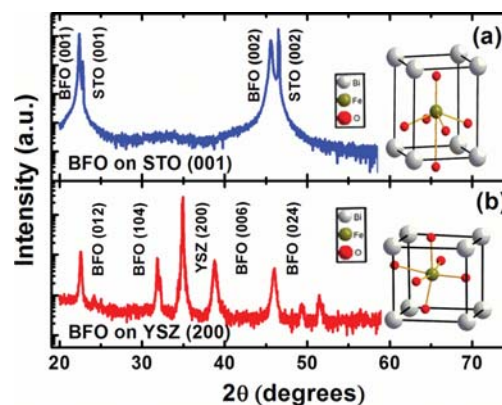


FIG. 1. (Color online) The x-ray diffraction pattern of the epitaxial growth BFO films on (a) (001)-STO and (b) (200)-YSZ. The insets illustrate the schematic drawing of the crystal structures.

^{a)}Authors to whom correspondence should be addressed. Electronic addresses: ghma@staff.shu.edu.cn and cheng@uow.edu.au.

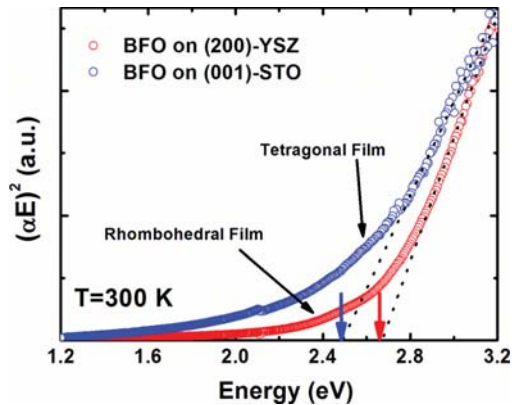


FIG. 2. (Color online) Variations in $(\alpha E)^2$ with the photon energy E are used to determine the optical band gap of the BFO films at room temperature.

the XRD pattern of the polycrystalline BFO films deposited on (001)-STO and (200)-YSZ, respectively. The film on (200)-YSZ is well crystallized with rhombohedral phase. This rhombohedrally distorted perovskite belongs to the R3c space group.^{3,7} Each Fe^{3+} center is coordinated by six O^{2-} ions, as shown in the inset of Fig. 1. The BFO film deposited on (001)-STO is crystallized with tetragonal phase. A slight tetragonal distortion reduces the space group to P4mm and modifies the overall perovskite structure, therefore the local Fe^{3+} environment is quasi-square pyramidal.^{7,25} One of the Fe-O axial distances increases to $\sim 2.80 \text{ \AA}$, and the Fe-O equatorial bond lengths are reduced to $\sim 1.93 \text{ \AA}$ owing to the structure strain and symmetry breaking.²⁵ The pure tetragonal phase with small monoclinic distortion can be stabilized by the large epitaxial strain.²⁶

Figure 2 displays the absorption spectrum of the tetragonal BFO film compared with that of the rhombohedral analog at room temperature. It is found that the band gap (E_g) of rhombohedral BFO film on (200)-YSZ substrate is to be $\sim 2.67 \text{ eV}$, which is about 0.2 eV larger than that of tetragonal BFO film on (001)-STO substrate ($E_g \sim 2.48 \text{ eV}$) by a linear extrapolation of an $(\alpha_0 E)^2$ versus E plots to zero. This result is consistent with the theoretical calculation, which predicts a smaller band gap in tetragonal BFO film.^{25,26}

The transient reflectivity changes reported here are performed by using a dual-color pump-probe technique. The light source is a commercial mode-locked Ti: sapphire laser (Spectra-Physics, Spitfire Pro.) operated at a repetition rate of 1 KHz , the pulse width of 120 fs , and the center wavelength of 800 nm . The output pulse train is split by an 8:2 beam splitter. After the beam splitter, the major part is frequency-doubled in a 1-mm BBO crystal as the pump beam of $\sim 1 \text{ mW}$ at the center wavelength of 400 nm (3.1 eV), the energy of which is larger than the band gap of BFO films. The fundamental with average power of $\sim 100 \mu\text{W}$ acts as the probe beam. Both of the pump and probe beams are focused on the surface of samples with near normal incidence. The pump beam is modulated at 490 Hz with a mechanic chopper. The reflected probe signal is detected by a photodiode connected with a lock-in amplifier to improve the signal to noise ratio. All experiments are performed at room temperature without any competing relaxation processes from the shift of energy gap or spin ordering at low temperature.^{27,28}

Figures 3(a) and 3(b) show the typical transient reflectivity changes ($\Delta R/R$) of BFO thin films on (001)-STO and (200)-YSZ substrates, respectively. The sharp increase around zero time delay in $\Delta R/R$ is corresponding to the excitation of hot electrons by the 400-nm pump pulse. The electron-electron (e-e) scattering is assumed to establish a thermal distribution of electrons on a time scale typically faster than the experimental time resolution. Therefore, following the initial rising, $\Delta R/R$ curves contain three successive relaxation processes. (1) The ultrafast component ($\sim 1 \text{ ps}$) corresponds to the e-ph interaction, which can be attributed to phonon thermalization through the anharmonic decay of optical phonons. (2) The subsequent slow component (\sim tens of ps) gives the information of energy exchange between the lattice and spin systems.^{29,30} These two processes can be described by a convolution of the Gaussian function $G(t)$ (laser pulse) with a bi-exponential decay function,

$$\Delta R/R = \left(A_1 \exp\left(-\frac{t}{\tau_{e-ph}}\right) + A_2 \exp\left(-\frac{t}{\tau_{s-ph}}\right) \right) \otimes G(t). \quad (1)$$

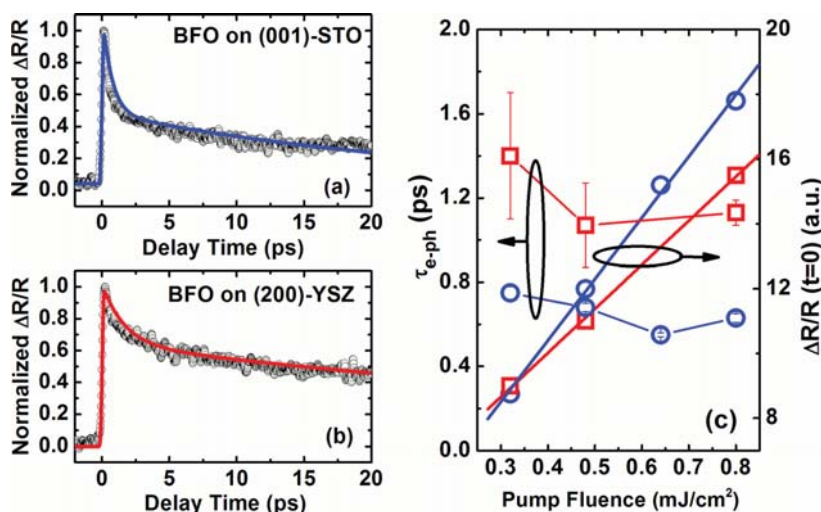


FIG. 3. (Color online) Normalized temporal evolution of differential reflectivity of (a) tetragonal and (b) rhombohedral BFO films on (001)-STO and (200)-YSZ, respectively. (c) Pump-fluence dependences of the peak amplitude of $\Delta R/R$ and τ_{e-ph} of tetragonal BFO film (blue circles) and rhombohedral one (red squares), respectively. The solid lines are guides to the eye.

where A_1 and A_2 are the amplitudes of the fast and slow components mentioned above, respectively. τ_{e-ph} and τ_{s-ph} are the relaxation time constants of the fast and slow components, respectively. Equation (1) is used to fit the experimental data (solid lines in Figs. 3(a) and 3(b)). (3) An oscillation component appears during the relaxation process in La and Nb codoping BFO films. But for the samples used in the present experiment, the oscillation component is too weak to be identified clearly, which will be presented in another publication including the information about s-ph coupling.

The relaxation time constants τ_{e-ph} of BFO films on STO and YSZ substrates with different crystalline orientations are extracted by fitting at a pump fluence of 0.8 mJ/cm^2 . It can be found that $\tau_{e-ph} \sim 0.6 \pm 0.01 \text{ ps}$ of tetragonal BFO film on (001)-STO is faster than $\tau_{e-ph} \sim 1.13 \pm 0.06 \text{ ps}$ of rhombohedral one on (200)-YSZ. Furthermore, the fit yields $\tau_{e-ph} \sim 1.31 \pm 0.07 \text{ ps}$ for rhombohedral BFO film on (110)-YSZ substrate, $\tau_{e-ph} \sim 0.58 \pm 0.04 \text{ ps}$ and $0.70 \pm 0.02 \text{ ps}$ for tetragonal BFO films on (110)-STO and (111)-STO substrates, respectively. Remarkably, the current result elucidates that τ_{e-ph} is almost independent with the crystalline orientations of the substrates, which suggests a moderate e-ph coupling strength for the same crystal system.

In general, the photo-excited electrons relaxation time in a metal is governed by thermalization of electrons through e-e scattering and transfer of energy from electron degrees of freedom to lattice degrees of freedom, referred to as the two-temperature model (TTM).^{15,16} The assumption behind TTM regime is that the relaxation time due to e-e collisions τ_{e-e} (\sim tens of fs) is much shorter than τ_{e-ph} , as a result, electron system and phonon system can be treated independently with characteristic temperature of T_e and T_l , respectively. A theoretical framework expressing τ_{e-ph} is related to the second moment of the Eliashberg function $\lambda\langle\omega^2\rangle = \frac{\pi}{3} \frac{k_B T_e}{\hbar \tau_{e-ph}}$, where $\langle\omega^2\rangle$ is a mean-square phonon frequency.^{19–21} This expression suggests that τ_{e-ph} is linearly dependent on temperature of electron T_e . However, in our case, τ_{e-ph} is virtually pump-fluence independent although the amplitude of the initial peak of $\Delta R/R$ at zero time delay shows a linear pump-fluence dependence, as shown in Fig. 3(c). In other words, TTM is not applicable for multiferroic materials.

Using the kinetic Boltzmann equation with e-e and e-ph collision integrals, the behavior of hot electrons relaxation can be re-considered, which has been done both theoretically and experimentally.^{20,21} The calculated electron distribution based on the analytical solution of this nonequilibrium model (NEM) deviates from the equilibrium Fermi-function particularly for high energies and yields $\lambda\langle\omega^2\rangle = \frac{2\pi}{3} \frac{k_B T_l}{\hbar \tau_{e-ph}}$.²¹ Since the heat capacity of the lattice in BFO films is much larger than that of electrons, then the lattice temperature T_l is close to room temperature for all fluences. Our data are consistent with the NEM expectation in poor metals without the assumption of $\tau_{e-e} \ll \tau_{e-ph}$. The e-ph coupling parameters can be estimated, $\lambda\langle\omega^2\rangle \sim 36.4$ and 66.7 meV^2 for rhombohedral BFO film on (200)-YSZ and tetragonal one on (001)-STO, respectively. The stronger e-ph coupling parameter of tetragonal BFO film, extracted from the interaction between microscopic degrees of freedom, could be regarded as giving rise to the strong electromechanical effect.^{8,24}

In summary, the ultrafast pump-probe spectroscopy is used to study the transient response of multiferroic BFO films with tetragonal and rhombohedral crystal structures. Hot electrons are photo-excited and relaxed with two different characteristic times. The fast process is attributed to the electron-lattice interaction, and the slow one is corresponding to the spin-lattice thermalization. The relaxation time constants τ_{e-ph} of tetragonal BFO films are faster than that of the rhombohedral ones, which suggests that the strength of e-ph interaction is enhanced by structural strain and symmetry breaking in tetragonal BFO films. The current experimental results indicate that crystal structure can be tuned to yield desired e-ph coupling properties, which is necessary for achieving predictive functionalities.

The research is supported by National Natural Science Foundation of China (11174195), Science and Technology Commission of Shanghai municipal (09530501100). Part of work was also supported Shanghai Leading Academic Discipline Project (S30105). Z. X. Cheng thanks the Australian Research Council for support through a Future Fellowship.

¹W. Eerenstein, N. D. Mathur, and J. F. Scott, *Nature* **442**, 759 (2006).

²K. Y. Yun, M. Noda, and M. Okuyama, *Appl. Phys. Lett.* **83**, 3981 (2003).

³J. Wang, J. B. Neaton, H. Zheng, V. Nagarajan, S. B. Ogale, B. Liu, D. Viehland, V. Vaithyanathan, D. G. Schlom, U. V. Waghmare *et al.*, *Science* **299**, 1719 (2003).

⁴Z. Cheng, X. Wang, S. Dou, H. Kimura, and K. Ozawa, *Phys. Rev. B* **77**, 092101 (2008).

⁵Z. Cheng and X. Wang, *Phys. Rev. B* **75**, 172406 (2007).

⁶S. R. Basu, L. W. Martin, Y. H. Chu, M. Gajek, R. Ramesh, R. C. Rai, X. Xu, and J. L. Musfeldt, *Appl. Phys. Lett.* **92**, 091905 (2008).

⁷P. Chen, N. J. Podraza, X. S. Xu, A. Melville, E. Vlahos, V. Gopalan, R. Ramesh, D. G. Schlom, and J. L. Musfeldt, *Appl. Phys. Lett.* **96**, 131907 (2010).

⁸R. J. Zeches, M. D. Rossell, J. X. Zhang, A. J. Hatt, Q. He, C.-H. Yang, A. Kumar, C. H. Wang, A. Melville, C. Adamo *et al.*, *Science* **326**, 977 (2009).

⁹K.-T. Ko, M. H. Jung, Q. He, J. H. Lee, C. S. Woo, K. Chu, J. Seidel, B.-G. Jeon, Y. S. Oh, K. H. Kim *et al.*, *Nat. Commun.* **2**, 567 (2011).

¹⁰D. S. Rana, I. Kawayama, K. Mavani, K. Takahashi, H. Murakami, and M. Tonouchi, *Adv. Mater.* **21**, 2881 (2009).

¹¹D. S. Rana, K. Takahashi, K. R. Mavani, I. Kawayama, H. Murakami, and M. Tonouchi, *Phys. Rev. B* **77**, 024105 (2008).

¹²A. Kumar, R. C. Rai, N. J. Podraza, S. Denev, M. Ramirez, Y. H. Chu, L. W. Martin, J. Ihlefeld, T. Heeg, J. Suchubert *et al.*, *Appl. Phys. Lett.* **92**, 121915 (2008).

¹³B. Gu, Y. Wang, J. Wang, and W. Ji, *Opt. Express* **17**, 10970 (2009).

¹⁴L. Y. Chen, J. C. Yang, H. C. Shih, C. W. Liang, T.-Y. Wu, S. K. Chou, C. W. Luo, K. H. Wu, Y. H. Chu, and T. Kobayashi, *J. Supercond. Novel Magn.* **24**, 731 (2011).

¹⁵H. E. Elsayed-Ali, T. B. Norris, M. A. Pessot, and G. A. Mourou, *Phys. Rev. Lett.* **58**, 1212 (1987).

¹⁶R. H. M. Groeneveld, R. Sprik, and A. Lagendijk, *Phys. Rev. B* **45**, 5079 (1992).

¹⁷A.-M. Dowgiallo and K. L. Knappenberger, Jr., *Phys. Chem. Chem. Phys.* **13**, 21585 (2011).

¹⁸H. Yan, D. Song, K. Fai Mak, I. Chatzakis, J. Maultzsch, and T. F. Heinz, *Phys. Rev. B* **80**, 121403(R) (2009).

¹⁹T. Tanedai, G. P. Pepe, L. Parlato, A. A. Golubov, and R. Sobolewski, *Phys. Rev. B* **75**, 174507 (2007).

²⁰V. V. Kabanov and A. S. Alexandrov, *Phys. Rev. B* **78**, 174514 (2008).

²¹C. Gadermaier, A. S. Alexandrov, V. V. Kabanov, P. Kusar, T. Mertelj, X. Yao, C. Manzoni, D. Brida, G. Cerullo, and D. Mihailovic, *Phys. Rev. Lett.* **105**, 257001 (2010).

²²L. Stojchevska, P. Kusar, T. Mertelj, V. V. Kabanov, X. Lin, G. H. Cao, Z. A. Xu, and D. Mihailovic, *Phys. Rev. B* **82**, 012505 (2010).

- ²³G. Schlom, L.-Q. Chen, C.-B. Eom, K. M. Rabe, S. K. Streiffer, and J.-M. Triscone, *Annu. Rev. Mater. Res.* **37**, 589 (2007).
- ²⁴H. Liu, P. Yang, K. Yao, K. P. Ong, P. Wu, and J. Wang, "Origin of a tetragonal BiFeO₃ phase with a giant c/a ratio on SrTiO₃ substrates," *Adv. Funct. Mater.* (2011).
- ²⁵H. M. Tütüncü and G. P. Srivastava, *Phys. Rev. B* **78**, 235209 (2008).
- ²⁶D. Ricinchi, K.-Y. Yun, and M. Okuyama, *J. Phys.: Condens. Matter* **18**, L97 (2006).
- ²⁷W. W. Li, J. J. Zhu, J. D. Wu, J. Gan, Z. G. Hu, M. Zhu, and J. H. Chu, *Appl. Phys. Lett.* **97**, 121102 (2010).
- ²⁸X. S. Xu, T. V. Brinzari, S. Lee, Y. H. Chu, L. W. Martin, A. Kumar, S. McGill, R. C. Rai, R. Ramesh, V. Gopalan *et al.*, *Phys. Rev. B* **79**, 134425 (2009).
- ²⁹Z. Jin, H. Ma, G. Li, Y. Xu, G. Ma, and Z. Cheng, *Appl. Phys. Lett.* **100**, 021106 (2012).
- ³⁰Y. Q. An, A. J. Taylor, S. D. Conradson, S. A. Trugman, T. Durakiewicz, and G. Rodriguez, *Phys. Rev. Lett.* **106**, 207402 (2011).